TEMPLE UNIVERSITY SAN LAB

Do You Feel What I Feel?

Developmental Differences in Emotion Representation

William Mitchell*, Lindsey Tepfer, Nicole Henninger, Susan Perlman, Vishnu Murty, Chelsea Helion

*Contact: Billy.Mitchell@temple.edu

Supplementary Information Sheet

Study Limitations: While our results suggest a number of differences in affective representation between children and adults, it is difficult to conclude with certainty exactly what implications this similarity has for cognition and behavior without additional measurements. Our interpretations of these results are based upon the extant literature exploring the functions of the AMY, NAcc, and vmPFC in similar experimental contexts, but the debate as to the exact functions of each is still widely contested. Meta-analyses suggest that the posterior vmPFC, for example, differentially responds to emotion, while the rostral and central vmPFC demonstrate increased activation during social processing and valuation judgments, respectively (Hiser & Koenigs, 2018).

Given the lack of statistical differences by valence among our adult sample in the vmPFC, there was concern that the patterns observed may be tracking non-affective constructs. To address this concern, we compared pattern similarity of all affective pairwise comparisons to pairwise comparisons of our neutral stimuli set. Representational similarity was far greater for affective stimuli than non-affective stimuli ($t(5993) = 6.96$, $p < 0.001$). However, this analysis cannot necessarily address concerns of social representations, as neutral stimuli were not as extensively balanced to positive and negative video stimuli and positive and negative video stimuli were to each other.

Task & Data Acquisition: *See* Karim & Perlman (2017),

Pre-Processing: Structural and functional data was preprocessed and high-pass filtered using the FEAT tool included in FSL (v5.0; https://fsl.fmrib.ox.ac.uk) (Jenkinson, Beckmann, & Behrens, 2012). Functional data were registered to anatomical and nonlinearly warped to MNI standard space. Timeseries data were extracted from CSF and white matter and used to identify motion-related deviations at each time point in order to isolate head motion, using six parameters, and other noise-related factors. Additionally, individual TRs were identified and adjusted for if greater than 15% of TRs were considered outliers, or if head motion values for any of the three rotations were greater than 1.5mm.

Figure 1: Stimuli clip examples from each film

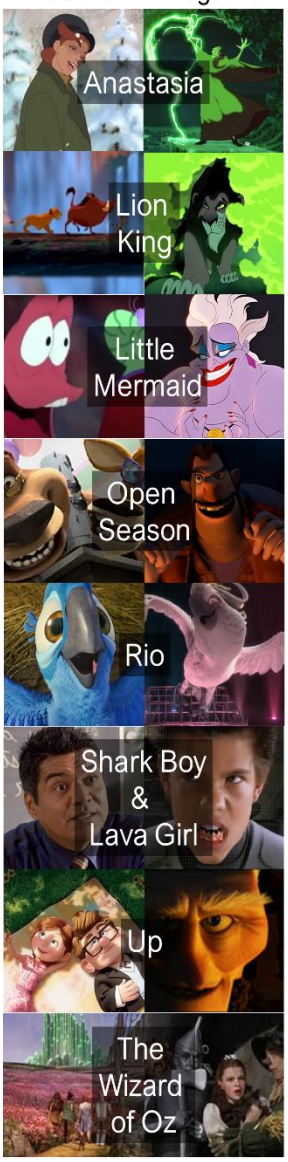

Regions of Interest: We captured vmPFC data using an activation-centered mask with a 2mm diameter isotropic kernel. Central MNI coordinates [X, Y, Z: 2, 46, -8] for the mask were identified in a meta-analysis by Barta, McGuire, and Kable (2013) as the most common center of consistent vmPFC activation during studies of subjective valuation and primary incentives. Amygdala and NAcc masks were taken from the Harvard-Oxford subcortical atlas (Makris et al., 2006; Frazier et al. 2005; Desikan et al., 2006; Goldstein et al., 2007). Masks were applied to all regions of interest (ROIs), such that data from voxels beyond the bounds of the masks were excluded, and the included voxels were aligned with functional volumes. All ROIs were thresholded at 50%. All masks were broadly defined in MNI space, applied to ROIs, and ROIs were transformed into subject native space using non-linear estimations (FNIRT). Transformations were visually inspected for accuracy.

Statistical Analyses: For each participant, we ran a General Linear Model (GLM) which had 16 regressors of interest, one for each valenced video clip. From these individual participant GLMs, we then extracted the activity for each voxel within each of our three ROIs (AMY, NAcc, and vmPFC) for each of the video clips. The value of each voxel represents the average change in activation while passively viewing the video stimulus relative to baseline fixation cross measurements. To measure representational similarity within each of our three ROIs, the individual

Table 1: Bonferroni-Adjusted Age Group & ROI Contrast

Contrasts	X Mean	Y Mean	Difference	SE	Lower 95% CI	Upper 95% CI	T Statistic	df	Unadjusted P Value	Bonferroni P Value
AMY , Child v. Adult	0.252	0.207	0.045	0.012	0.021	0.07	3.64	2502	> 0.001 ***	> 0.001 ***
NAcc , Child v. Adult	0.292	0.225	0.067	0.016	0.035	0.099	4.068	2371	> 0.001 ***	> 0.001 ***
vmPFC , Child v. Adult	0.349	0.224	0.125	0.017	0.092	0.158	7.366	2465	> 0.001 ***	> 0.001 ***
AMY v. Nacc, Child	0.252	0.292	-0.04	0.014	-0.067	-0.012	-2.834	2705	0.005 **	0.085
AMY v. vmPFC, Child	0.252	0.349	-0.097	0.015	-0.126	-0.068	-6.536	2607	> 0.001 ***	> 0.001 ***
NAcc v. vmPFC, Child	0.292	0.349	-0.057	0.016	-0.088	-0.026	-3.571	2776	> 0.001 ***	> 0.001 ***
AMY v. Nacc, Adult	0.207	0.225	-0.018	0.015	-0.048	0.011	-1.209	2005	0.227	1.000
AMY v. vmPFC, Adult	0.207	0.224	-0.017	0.015	-0.046	0.012	-1.136	2018	0.256	1.000
NAcc v. vmPFC, Adult	0.225	0.224	0.001	0.017	-0.033	0.035	0.072	2238	0.942	1.000
AMY, Child & NAcc, Adult v. AMY, Adult & NAcc, Child	0.24	0.254	-0.014	0.01	-0.034	0.006	-1.351	5033	0.177	1.000
AMY, Child & vmPFC, Adult v. AMY, Adult & vmPFC, Child	0.239	0.286	-0.047	0.011	-0.067	-0.025	-4.327	5026	> 0.001 ***	> 0.001 ***
Nacc, Child & vmPFC, Adult v. Nacc, Adults & vmPFC, Child	0.294	0.261	0.033	0.012	0.009	0.055	2.723	5018	0.006 **	0.102

Table 2: Bonferroni-Adjusted Age Group & Valence Contrast

Contrasts	X Mean	Y Mean	Difference	SE	Lower 95% CI	Upper 95% CI	T Statistic	df	Raw P Value	Bonferroni P Value
Positive v. Negative, Adult	0.223	0.214	0.009	0.013	-0.016	0.035	0.727	3358	0.467	1.000
Positive v. Negative, Child	0.272	0.323	-0.051	0.012	-0.075	-0.027	-4.142	4196	> 0.001 ***	> 0.001 ***
Child v. Adult, Positive	0.272	0.223	0.049	0.013	0.024	0.074	3.872	3687	> 0.001 ***	> 0.001 ***
Child v. Adult, Negative	0.323	0.214	0.109	0.013	0.084	0.134	8.693	3660	> 0.001 ***	> 0.001 ***
Child, Positive & Adult, Negative v. Adult, Positive & Child, Negative	0.278	0.246	0.032	0.009	0.015	0.05	3.613	7558	> 0.001 ***	> 0.001 ***

voxels contained within each participant's GLM were aligned by MNI coordinates, such that the same spaces were being compared to one another within-participant across clips.

Next, we used representational similarity analysis (RSA) to calculate our dependent measure. Pairwise complete observations of activity in each voxel within each ROI for each video clip were correlated with one another using the Spearman rank-order correlation method for non-parametric data. Pairwise comparisons were performed across movie, but within valenced movie clips for each participant. This system produces an equal number of correlations in two within-valence categories: positive-to-positive comparisons and negative-to-negative comparisons. Fisher's Z-Transformation was applied to all correlations before proceeding. Correlating the extracted GLM data from our 8 positive movie clips and 8 negative movie clips produced 28 correlative coefficients for within-valence comparisons per participant per ROI.

Analyses were performed using the R statistical programming language (v4.0.3; http://www.R-project.org/) in conjunction with the Integrated Development Environment, RStudio (v1.3.1093; https://rstudio.com/)

References:

Bartra, O., McGuire, J. T., & Kable, J. W. (2013). The valuation system: A coordinate-based meta-analysis of BOLD fMRI experiments examining neural correlates of subjective value. *NeuroImage*, *76*, 412–427.

Desikan, R. S., Fischl, B., Quinn, B. T., Dickerson, B. C., Blacker, D., Buckner, R. L., Dale, A. M., Maguire, R. P., Hyman, B. T., Albert, M. S., & Killiany, R. J. (2006). An automated labeling system for subdividing the human cerebral cortex on MRI scans into gyral based regions of interest. *Neuroimage*, *31*(3), 968–980.

Frazier, J. A., Chiu, S., Breeze, J. L., Makris, N., Lange, N., Kennedy, D. N., Herbert, M. R., Bent, E. K., Koneru, V. K., Hodge, S. M., Rauch, S. L., Grant, P. E., Cohen, B. M., Seidman, L. J., Caviness, V. S., & Biederman, J. (2005). Structural brain magnetic resonance imaging of limbic and thalamic volumes in pediatric bipolar disorder. *American Journal of Psychiatry*, *162*(7), 1256–1265.

Gee, D. G., Humphreys, K. L., Flannery, J., Goff, B., Telzer, E. H., Shapiro, M., Hare, T. A., Bookheimer, S. Y., & Tottenham, N. (2013). A Developmental Shift from Positive to Negative Connectivity in Human Amygdala-Prefrontal Circuitry. *Journal of Neuroscience*, *33*(10), 4584–4593.

Goldstein, J. M., Seidman, L. J., Makris, N., Ahern, T., O'Brien, L. M., Caviness, V. S., Kennedy, D. N., Faraone, S. V., & Tsuang, M. T. (2007). Hypothalamic abnormalities in schizophrenia: Sex effects and genetic vulnerability. *Biological Psychiatry*, *61*(8), 935–945.

Hiser, J., & Koenigs, M. (2018). The Multifaceted Role of the Ventromedial Prefrontal Cortex in Emotion, Decision Making, Social Cognition, and Psychopathology. *Biological Psychiatry*, *83*(8), 638–647.

Jenkinson, M., Beckmann, C. F., Behrens, T. E. J., Woolrich, M. W., & Smith, S. M. (2012). FSL. *NeuroImage*, *62*(2), 782–790.

Karim, H. T., & Perlman, S. B. (2017). Neurodevelopmental maturation as a function of irritable temperament. *Human Brain Mapping*, *38*(10), 5307–5321.

Makris, N., Goldstein, J. M., Kennedy, D., Hodge, S. M., Caviness, V. S., Faraone, S. V., Tsuang, M. T., & Seidman, L. J. (2006). Decreased volume of left and total anterior insular lobule in schizophrenia. *Schizophrenia Research*, *83*(2–3), 155–171.